

Non-equilibrium renormalised contacts for transport in nanodevices with interaction: a quasi-particle approach

H. Ness, L. K. Dash

Department of Physics, University of York, Heslington, York YO10 5DD, UK
European Theoretical Spectroscopy Facility (ETSF)

Abstract. We present an application of a new formalism to treat the quantum transport properties of fully interacting nanoscale junctions. We consider a model single-molecule nanojunction in the presence of two kinds of electron-vibron interactions. In terms of the electron density matrix, one interaction is diagonal in the central region and the second off-diagonal between the central region and the left electrode. We use a non-equilibrium Green's function technique to calculate the system's properties in a self-consistent manner. The interaction self-energies are calculated at the Hartree-Fock level in the central region and within a dynamical mean-field-like approach for the crossing interaction. Our calculations are performed for different transport regimes ranging from the far off-resonance to the quasi-resonant regime, and for a wide range of parameters. They show that a non-equilibrium (i.e. bias dependent) dynamical (i.e. energy dependent) renormalisation is obtained for the contact between the left electrode and the central region in the form of a non-equilibrium renormalisation of the lead embedding potential. The conductance is affected by the renormalisation of the contact: the amplitude of the main resonance peak is modified as well as the lineshape of the first vibron side-band.

PACS numbers: 73.40.Gk, 71.38.-k, 73.63.-b, 85.65.+h

1. Introduction

The theory of quantum electronic transport in nano-scale devices has evolved rapidly over the past decade, as advances in experimental techniques have made it possible to measure transport properties down to single-molecule devices. The development of accurate theoretical methods for the description of quantum transport at the single-molecule level is essential for continued progress in a number of areas including molecular electronics, spintronics, and thermoelectrics [1].

One of the longstanding problems in quantum charge transport is the establishment of a theoretical framework which allows for quantitatively accurate predictions of conductance from first principles. The need for methods going beyond the conventional approaches, based on equilibrium electronic structure calculations combined with Landauer-like elastic scattering, has been clear for a number of years. Only recently have more advanced methods to treat electronic interaction appeared (for example see Refs. [2, 3, 4]).

Alternative frameworks to deal with the steady-state or time-dependent transport are given by many-body perturbation theory, based on the non-equilibrium (NE) Green's function (GF) formalism: in these approaches, the interactions and (initial) correlations are taken into account by using conserving approximations for the many-body self-energy [5, 6, 7, 8, 9, 10, 11, 12, 13, 14].

Other interactions, such as electron-phonon coupling, also play an important role in single-molecule quantum transport. These interactions are more important in nanoscale systems, as the electronic probability density is concentrated in a small region of space and thus normal screening mechanisms are ineffective. Such interactions are also crucial in inelastic electron tunneling spectroscopy. Such a technique constitutes an important basis for spectroscopy of molecular junctions, yielding insight into the vibrational modes (single molecule phonons called vibrons) and ultimately the atomic structure of the junction [15].

There have been many theoretical investigations focusing on the effect of electron-vibron coupling in molecular- and atomic-scale wires [16-51]. In all these studies, the interactions have always been considered to be present in the central region (i.e. the molecule) only, with the latter connected to two non-interacting terminals. Interactions are also assumed not to cross at the contacts between the central region and the leads. When electronic interactions are present throughout the system, as within density-functional theory calculations, they are treated only at the mean-field level and do not allow for any inelastic scattering events. However, such approximations are valid only in a very limited number of practical cases. The interactions, in principle, exist throughout the entire system.

In a recent paper we derived a general expression for the current in nano-scale junctions with interaction present everywhere in the system [52]. The importance of such extended interactions in nano-scale devices has also been addressed, for electron-electron interaction, in recently developed approaches such as Refs. [2, 53].

In the present paper, we apply our formalism [52] to a specific model of single-molecule nanojunctions. We focus on a model system in the presence of electron-vibron interaction both within the molecule *and* between the molecule and one of the leads. We adopt a quasiparticle-like approach to treat the crossing interactions (i.e. there are some restrictions on the components of the self-energy for the crossing interaction). We show how the interaction crossing at one interface of the molecular nanojunctions affects the transport properties by renormalising the coupling at the interface in a dynamical and bias-dependent manner.

The paper is organised as follows: In Sec. 2, we briefly recall the main result of our expression for the current in fully interacting systems. In Sec. 3, we present the model Hamiltonian for the system which includes two kinds of electron-vibron interaction: a Holstein-like Hamiltonian combined with a Su-Schrieffer-Heeger-like Hamiltonian. In this section, we also describe how the corresponding self-energies are calculated and the implications of such approximations on the current expression at the left and right interfaces. In Sec. 4, we show how the non-equilibrium dynamical renormalisation affects the generalised embedding potential of the left (L) lead, and how in turn this affects the conductance of the nanojunction. We finally conclude and discuss extensions of the present work in Sec. 5.

2. General theory for quantum transport

We consider a two-terminal device, made of three regions left-central-right, labelled $L - C - R$, in the steady-state regime. In such a device the interaction—which we specifically leave undefined (e.g. electron-electron or electron-phonon)—is assumed to be well described in terms of the single-particle self-energy Σ^{MB} and spreads throughout the entire system.

We use a compact notation for the Green's function G and the self-energy Σ matrix elements $M(\omega)$. They are annotated M_C (M_L or M_R) for the elements in the central region C (left L , right R region respectively), and M_{LC} (or M_{CL}) and M_{RC} (or M_{CR}) for the elements between region C and region L or R . There are no direct interactions between the two electrodes, i.e. $\Sigma_{LR/RL}^{\text{MB}} = 0$.

In Refs. [52, 54], we showed that for a finite applied bias V the steady-state current $I_L(V)$ flowing through the left LC interface is given by:

$$\begin{aligned}
 I_L = & \frac{e}{\hbar} \int \frac{d\omega}{2\pi} \text{Tr}_{\{C\}} \left[G_C^r \tilde{\Upsilon}_C^{L,l} + G_C^a (\tilde{\Upsilon}_C^{L,l})^\dagger + G_C^< (\tilde{\Upsilon}_C^L - (\tilde{\Upsilon}_C^L)^\dagger) \right] \\
 & + \text{Tr}_{\{L\}} \left[\Sigma_L^{\text{MB},>} G_L^< - \Sigma_L^{\text{MB},<} G_L^> \right]
 \end{aligned} \tag{1}$$

where the $\tilde{\Upsilon}_C^X$ quantities are

$$\begin{aligned}
 \tilde{\Upsilon}_C^L(\omega) &= \Sigma_{CL}^a(\omega) \tilde{g}_L^a(\omega) \Sigma_{LC}^r(\omega), \\
 (\tilde{\Upsilon}_C^L)^\dagger &= \Sigma_{CL}^a \tilde{g}_L^r \Sigma_{LC}^r, \\
 \tilde{\Upsilon}_C^{L,l} &= \Sigma_{CL}^< (\tilde{g}_L^a - \tilde{g}_L^r) \Sigma_{LC}^r + \Sigma_{CL}^r \tilde{g}_L^< \Sigma_{LC}^r.
 \end{aligned} \tag{2}$$

By definition $\Sigma_{LC}(\omega) = V_{LC} + \Sigma_{LC}^{\text{MB}}(\omega)$ (similarly for the CL components) where $V_{LC/CL}$ are the nominal coupling matrix elements between the L and C regions. $\tilde{g}_L^x(\omega)$ are the GF of the region L renormalised by the interaction *inside* that region, where $x = r, a, <$ stands for the retarded, advanced and lesser GF components respectively. For example, for the advanced and retarded components, we have $(\tilde{g}_L^{r/a}(\omega))^{-1} = (g_L^{r/a}(\omega))^{-1} - \Sigma_L^{\text{MB},r/a}(\omega)$ where all quantities are defined only in the subspace L .

The second trace in Eq. (1) corresponds to inelastic events induced by the interaction in the L lead. At equilibrium, because of the detailed balance equation $\Sigma^>G^< = \Sigma^<G^>$, this term vanishes. At non-equilibrium, this is generally not the case. However, when a local detailed balance equation holds, i.e. the system is locally in a (quasi)equilibrium state, this term vanishes since one recovers locally $\Sigma^{\text{MB},>}G^< = \Sigma^{\text{MB},<}G^>$. Hence, in practice, we do not have to worry about the infinite sum in the trace $\text{Tr}_{\{L\}}[\dots]$ since there will always be a region/boundary in the left lead L beyond which the system is at (quasi)equilibrium.

The first trace in the current equation Eq. (1) corresponds to a generalisation of the result of Meir and Wingreen [55]. It encompasses the cases for which the interactions are present in the three L, C, R regions as well as in between the L/C and C/R regions. It also bears some resemblance to the expression derived by Meir and Wingreen [55] when written as:

$$I_L^{\text{MW}} = \frac{e}{\hbar} \int \frac{d\omega}{2\pi} \text{Tr}_{\{C\}} \left[G_C^r \Sigma_C^{L,<} + G_C^a (\Sigma_C^{L,<})^\dagger + G_C^< (\Sigma_C^{L,a} - \Sigma_C^{L,r}) \right]. \quad (3)$$

where we use the standard definitions $\Sigma_C^{L,<} = -(\Sigma_C^{L,<})^\dagger = V_{CL} g_L^< V_{LC} = i f_L \Gamma_L$ and $\Sigma_C^{L,a} - \Sigma_C^{L,r} = V_{CL} (g_L^a - g_L^r) V_{LC} = i \Gamma_L$.

By comparing Eq. (1) and Eq. (3), we can see that the quantities $\tilde{\Upsilon}_{LC}$ ($\tilde{\Upsilon}_{LC}^\dagger$) and $\tilde{\Upsilon}_{LC}^l$ are now playing the role of the L lead self-energy Σ_L^a (Σ_L^r) and $\Sigma_L^<$ respectively when the interactions cross at the LC interface.

3. Model for the interaction

3.1. Hamiltonians

We consider a single-molecule junction in the presence of electron-vibron interaction both inside the central region and crossing at the contacts. We further concentrate on a model for the central region which consists of a single molecular level coupled to a single vibrational mode. A full description of our methodology, for the interaction inside the region C , is provided in Refs. [56, 57, 58]. Moreover, we consider that some electron-vibron interaction exists also at one contact (the left L electrode for instance). This model typically corresponds to an experiment for a molecule chemisorbed onto a surface (the left electrode) with a tunneling barrier to the right R lead.

In the following model, we consider two kinds of electron-vibron coupling: a local coupling in the sense of a Holstein-like coupling of the electron charge density with an internal degree of freedom of vibration inside the central region, and an off-diagonal

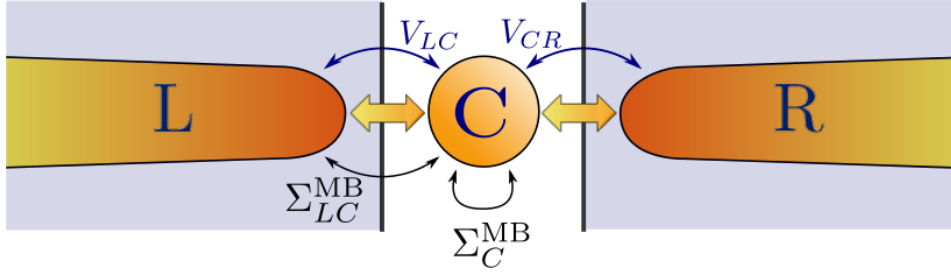


Figure 1. (Color online) Schematic representation of a central scattering region C connected to the left L and right R electrodes. Interactions are given by the coupling of the region C to the L (R) electrode ($V_{LC/CL}$ and $V_{RC/CR}$), and by the many-body effects within the central region (Σ_C^{MB}) and at the LC interface (Σ_{LC}^{MB}). Σ_C^{MB} corresponds to the coupling of an electron with the vibron mode ω_0 (with coupling strength γ_0), and Σ_{LC}^{MB} corresponds to the coupling of a hopping electron with another vibron mode ω_A (with coupling strength γ_A).

coupling in the sense of a Su-Schrieffer-Heeger-like coupling [59, 17] to another vibration mode involving the hopping of an electron between the central C region and the L electrode. A schematic representation of the molecular junction is given in Figure 1.

The Hamiltonian for the region C is

$$H_C = \varepsilon_0 d^\dagger d + \hbar\omega_0 a^\dagger a + \gamma_0 (a^\dagger + a) d^\dagger d, \quad (4)$$

where d^\dagger (d) creates (annihilates) an electron in the molecular level ε_0 . The electron charge density in the molecular level is coupled to the vibration mode of energy ω_0 via the coupling constant γ_0 , and a^\dagger (a) creates (annihilates) a vibration quantum in the vibron mode ω_0 . The central region C is nominally connected to two (left and right) one-dimensional tight-binding chains via the hopping integral t_{0L} and t_{0R} . The corresponding electrode $\alpha = L, R$ self-energy is $\Sigma_\alpha^r(\omega) = t_{0\alpha}^2 e^{ik_\alpha(\omega)} / \beta_\alpha$ with the dispersion relation $\omega = \varepsilon_\alpha + 2\beta_\alpha \cos(k_\alpha(\omega))$ where ε_α and β_α are the tight-binding on-site and off-diagonal elements of the electrode chains.

To describe the electron-vibron interaction existing across the left contact, we consider that the hopping integral t_{0L} is actually dependent on some generalised coordinate X . The latter represents either the displacement of the centre-of-mass of the molecule or of some chemical group at the end of the molecule link to the L electrode. At the lowest order, the matrix element can be linearised as $t_{0L}(X) = t_{0L} + t'_{0L}X$. Hence the hopping of an electron from the C region to the L region (and *vice versa*) is coupled to a vibration mode (of energy ω_A) via the coupling constant γ_A (itself related to t'_{0L}). The corresponding Hamiltonian is given by

$$H_{LC} = \gamma_A (b^\dagger + b) (c_L^\dagger d + d^\dagger c_L) + \omega_A b^\dagger b, \quad (5)$$

where b^\dagger (b) creates (annihilates) a vibration quantum in the vibron mode ω_A , the generalised coordinate is $X = \sqrt{\hbar/(2m_A\omega_A)}(b^\dagger + b)$, and c_L^\dagger (c_L) creates (annihilates) an electron in the level ε_L of the L electrode.

The Hamiltonians Eq. (4) and Eq. (5) are used to calculate the corresponding electron self-energies at different orders of the interaction γ_0 and γ_A using conventional non-equilibrium diagrammatic techniques [56, 58].

Furthermore, at equilibrium, the whole system has a single and well-defined Fermi level μ^{eq} . A finite bias V , applied across the junction, lifts the Fermi levels as $\mu_{L,R} = \mu^{\text{eq}} + \eta_{L,R}eV$. The fraction of potential drop [60] at the left contact is η_L and $\eta_R = \eta_L - 1$ at the right contact, with $\mu_L - \mu_R = eV$ and $\eta_L \in [0, 1]$.

3.2. Self-energies for the interactions

In this paper, we consider different approximations to treat the interaction inside the central region and the interaction crossing at the left contact. First of all, calculating exactly the corresponding interaction self-energies is a tremendous task since, in principle, they depend on both the phonon propagator and the electron Green's functions in all the different parts of the system. Hence, for the first application of our formalism, we proceed step by step in terms of the increasing complexity of the interaction; and we limit ourselves to approximations for the self-energies that are well known and well controlled.

The electron-vibron self-energies in the central region C are calculated within the self-consistent Born approximation (i.e. diagrams with one phonon line). The details of these calculations have been reported elsewhere [56, 58]. For the crossing interaction, we consider a mean-field-like approach for the electron-vibron coupling at the LC interface. Within such an approximation, we can understand the results of the calculations in terms of renormalisation of the LC contact.

Furthermore considering the crossing interaction occurring only at one interface permit us to check and test the consistency of our formalism. Indeed, with no interaction crossing at the right CR interface, the current I_R is given by the conventional Meir and Wingreen formula, i.e. Eq. (3) for the CR interface. In order to have a consistent formalism, we need to have current conservation, and such a constraint is best tested with crossing interaction at only one interface. The corresponding results are shown in detail in 4.1.

Within mean-field-like approximations, the effects of the crossing interaction correspond to a renormalisation of the coupling in a static or a dynamical manner. The corresponding self-energies have only retarded and advanced components $\Sigma_{LC}^{r/a}$ and $\Sigma_{CL}^{r/a}$. The extra inelastic effects included in the components Σ_{CL}^{\lessgtr} are neglected altogether.

Hence the Υ_C^X quantities defined in Eq. (2) become:

$$\begin{aligned}
 \tilde{\Upsilon}_C^L &= \Sigma_{CL}^a g_L^a \Sigma_{LC}^r, \\
 (\tilde{\Upsilon}_C^L)^\dagger &= \Sigma_{CL}^a g_L^r \Sigma_{LC}^r, \\
 \tilde{\Upsilon}_C^{L,l} &= \Sigma_{CL}^r g_L^< \Sigma_{LC}^r, \\
 (\tilde{\Upsilon}_C^{L,l})^\dagger &= -\Sigma_{CL}^a g_L^< \Sigma_{LC}^a.
 \end{aligned} \tag{6}$$

with $\Sigma_{LC}^{r/a} = V_{LC} + \Sigma_{LC}^{\text{MB},r/a}$.

Correspondingly, the generalised embedding potentials for the left contact defined as $Y_C^{L,x} = [\Sigma_{CL}^r g_L \Sigma_{LC}^r]^x$ [52, 54] with $x = r, a, \gtrless$, are now given by

$$\begin{aligned} Y_C^{L,r}(\omega) &= \Sigma_{CL}^r g_L^r \Sigma_{LC}^r, \\ Y_C^{L,a}(\omega) &= \Sigma_{CL}^a g_L^a \Sigma_{LC}^a, \\ Y_C^{L,<}(\omega) &= \Sigma_{CL}^r g_L^< \Sigma_{LC}^a. \end{aligned} \quad (7)$$

In the static limit, the mean-field approach leads to the Hartree expression for the electron-vibron self-energies at the LC interface:

$$\Sigma_{LC}^{\text{MB},r/a} = -2 \frac{\gamma_A^2}{\omega_A} \langle n_{LC} \rangle, \quad (8)$$

where

$$\langle n_{LC} \rangle = -i \int \frac{d\omega}{2\pi} G_{LC}^<(\omega). \quad (9)$$

The self-energy $\Sigma_{LC}^{\text{MB},r/a}$ is independent of the energy ω and leads to a static (nonetheless bias-dependent) renormalisation of the nominal coupling $V_{CL} = V_{LC} = t_{0L}$ between the L and C regions. This NE renormalisation will induce, among other effects, a bias-dependent modification of the broadening of the spectral features of the C region. We have analysed these effects in details in Ref.[51]. The renormalisation is such that the amplitude of the current is reduced in comparison with the current values obtained when the interaction is present only in the central region. The NE static renormalisation of the contact is highly non-linear and non-monotonic in function of the applied bias, and the larger effects occur at applied biases corresponding to resonance peaks in the dynamical conductance. The conductance is also affected by the NE renormalisation of the contact, showing asymmetric broadening around the resonance peaks and some slight displacement of the peaks at large bias in function of the coupling strength γ_A .

Beyond the static limit, we can develop a dynamical mean-field-like approach for the electron-vibron coupling following Ref. [62]. The retarded self-energy containing all orders of the electron-vibron coupling is expressed as a continued fraction as shown analytically in Refs. [63, 64]. We have already used such an approach to study the transport properties of organic molecular wires which are dominated by the propagation of polarons [16, 17] or solitons [18]. The expression for the corresponding self-energy $\Sigma_{LC}^r(\omega)$ is given by:

$$\Sigma_{LC}^r(\omega) = \frac{\gamma_A^2}{G_{LC}^r(\omega - \omega_A)^{-1} - \frac{2\gamma_A^2}{G_{LC}^r(\omega - 2\omega_A)^{-1} - \frac{3\gamma_A^2}{G_{LC}^r(\omega - 3\omega_A)^{-1} - \dots}} \quad (10)$$

where G_{LC}^r is the retarded component of the off-diagonal GF between the central region and the left lead L . Its closed expression is obtained from the corresponding Dyson

equation $G_{LC}^r = [g\Sigma G]_{LC}^r$:

$$G_{LC}^r(\omega) = \left[[g_L^r]^{-1} - \Sigma_{LC}^r \left[[\tilde{g}_C^r]^{-1} - Y_C^{R,r} \right]^{-1} \Sigma_{CL}^r \right]^{-1} \Sigma_{LC}^r \left[[\tilde{g}_C^r]^{-1} - Y_C^{R,r} \right]^{-1}, \quad (11)$$

with $\tilde{g}_C^r(\omega) = [\omega - \varepsilon_0 - \Sigma_C^{\text{MB},r}(\omega)]^{-1}$ and $Y_C^{R,r}(\omega) = V_{CR}g_R^r(\omega)V_{RC}$.

Such a dynamical mean-field-like approach, which corresponds to a quasi-particle approach since the self-energy $\Sigma_{LC/CL}^{r/a}$ can be incorporated into a Schrödinger-like equation, is expected to affect the transport properties via the non-equilibrium dynamical renormalisation of the contacts, i.e. through the generalised embedding potentials $Y_C^{L,x}(\omega)$ as well as through the corresponding $\Upsilon_C^x(\omega)$ quantities.

Finally, note that for the lowest-order expansion, the self-energy Σ_{LC}^r takes a simple form:

$$\Sigma_{LC}^r(\omega) = \gamma_A^2 G_{LC}^r(\omega - \omega_A). \quad (12)$$

4. Results

We have performed calculations, in a self-consistent manner, for many different values of the Hamiltonian parameters. We present below the most characteristic results for different transport regimes and for different coupling strengths γ_A , while the interaction in the region C is taken to be in the intermediate coupling regime $\omega_0 = 0.2$, $\gamma_0 = 0.15$, i.e. $\gamma_0/\omega_0 = 0.75$.

The nominal couplings between the central region and the electrodes $t_{0L,R}$, before NE renormalisation, are not too large, so that we can discriminate clearly between the different vibron side-band peaks in the spectral functions. The values chosen for the parameters are typical values for realistic molecular junctions [65, 58]. In the following the current is given in units of charge per time, the conductance in units of the quantum of conductance $G_0 = 2e^2/\hbar$ and the bias V and the embedding potential Y_C in natural units of energy where $e = 1$ and $\hbar = 1$.

4.1. Conserving approximation

One of the most important physical conditions that our formalism needs to fulfil is the constraint of current conservation. We use conserving approximations to calculate the interaction self-energies in the central region C and a quasi-particle approximation for crossing interaction at the left interface.

With our choice for $\Sigma_{LC}^r(\omega)$ given by Eq. (10), we find that the left lead generalised embedding potential $Y_C^{L,r}(\omega)$ is renormalised by the crossing interaction. This is clearly seen in Figure 2, which shows the imaginary part of $Y_C^{L,r}$ for different transport regimes, different coupling at the LC interface and for both equilibrium and non-equilibrium conditions.

At equilibrium, and in the absence of contact renormalisation, the imaginary part of $Y_C^{L,r}$ is simply the imaginary part of the conventional L lead self-energy

$\Sigma_L^r(\omega) = t_{0L}^2 e^{ik_L(\omega)} / \beta_L$ and corresponds to a semi-elliptic functions with non-zero values within the energy range $-2\beta_L \leq \omega \leq +2\beta_L$ (see dashed lines in figure 2). The spectral weight of $\Im m \Sigma_L^r$ is given by $\int d\omega \Im m \Sigma_L^r(\omega) = t_{0L}^2 \int d\omega \Im m g_L^r(\omega) = -\pi t_{0L}^2$.

In the presence of the renormalised L contact, we obtained a strong deviation from the semi-elliptic function as shown by the (red) thin lines and (black) thick lines in Figure 2, which correspond respectively to the equilibrium (bias $V = 0$) and the non-equilibrium (bias $V = 1.0$) conditions. This result indicates a strong reduction of the available transport channels in the renormalised L lead embedding potential for regions of energy where $\Sigma_{LC/LC}^{r/a}(\omega)$ has non-zero value.

However, a very important property is that the total spectral weight of $\Im m \Sigma_L^r$ is conserved for all the calculations we have performed, i.e. for all the different transport regimes, coupling strength γ_A and ω_A at the LC interface and all applied bias. We find that in all the cases $\int d\omega \Im m Y_C^{L,r}(\omega) = -\pi t_{0L}^2$ (with maximum deviation of 0.05% arising from numerical errors in the results shown in Figure 2). So in this sense, we can say that the approximation for $\Sigma_{LC/LC}^{r,a}$ is conserving.

Correspondingly, we have also carefully checked that the current is conserved for all the calculations presented in the present paper, i.e. that $|I_L + I_R| / |I_L| \sim |I_L + I_R| / |I_R| < 10^{-5}$, with the current I_L at the LC interface is given by expression Eq. (1) and the current I_R at the CR interface does not contain any contact renormalisation, and hence is given by a Meir and Wingreen like expression Eq. (3).

4.2. Dynamical non-equilibrium renormalisation

The dynamical renormalisation of the L lead embedding potential $Y_C^{L,r}$ presents features (dips) at some energies. Qualitatively speaking, there is a form of correlation between them and the features that exist in the spectral function of the central region $A_C(\omega) = (G_C^a(\omega) - G_C^r(\omega)) / 2\pi i$.

Figure 3 shows the spectral function $A_C(\omega)$, rescaled by some factor, for a set of parameters corresponding to panel (a) in figure 2. The bottom panel of figure 3 shows the imaginary part of $Y_C^{L,r}(\omega)$ from which the semi-elliptic background has been subtracted, i.e. $\Delta Y_C^{L,r} = Y_C^{L,r} - \Sigma_L^r$. Qualitatively speaking, both quantities present similar features, shifted in energy by an amount corresponding to ω_A ($\omega_A = 0.2$ in the calculations) as expected from the definition of $\Sigma_{LC/LC}^{r/a}(\omega)$.

One can then expect a maximum effect of the dynamical renormalisation in an integrated quantity such as the current when the features in $Y_C^{L,r}(\omega)$ coincide with those in the spectral function $A_C(\omega)$ within a given bias energy-window.

We now consider the modification of the dynamical conductance $G(V) = dI/dV$ induced by the crossing interaction $\Sigma_{LC/LC}^{r/a}(\omega)$ for different transport regimes and for different crossing interaction strength. Figures 4 and 5 show $G(V)$ for three different transport regimes for weak to strong crossing interaction strength γ_A , and for two values of ω_A ($\omega_A = 0.2$ for Fig. 4 and $\omega_A = 0.1$ Fig. 5).

The dynamical renormalisation of the left contact slightly affects the main resonance

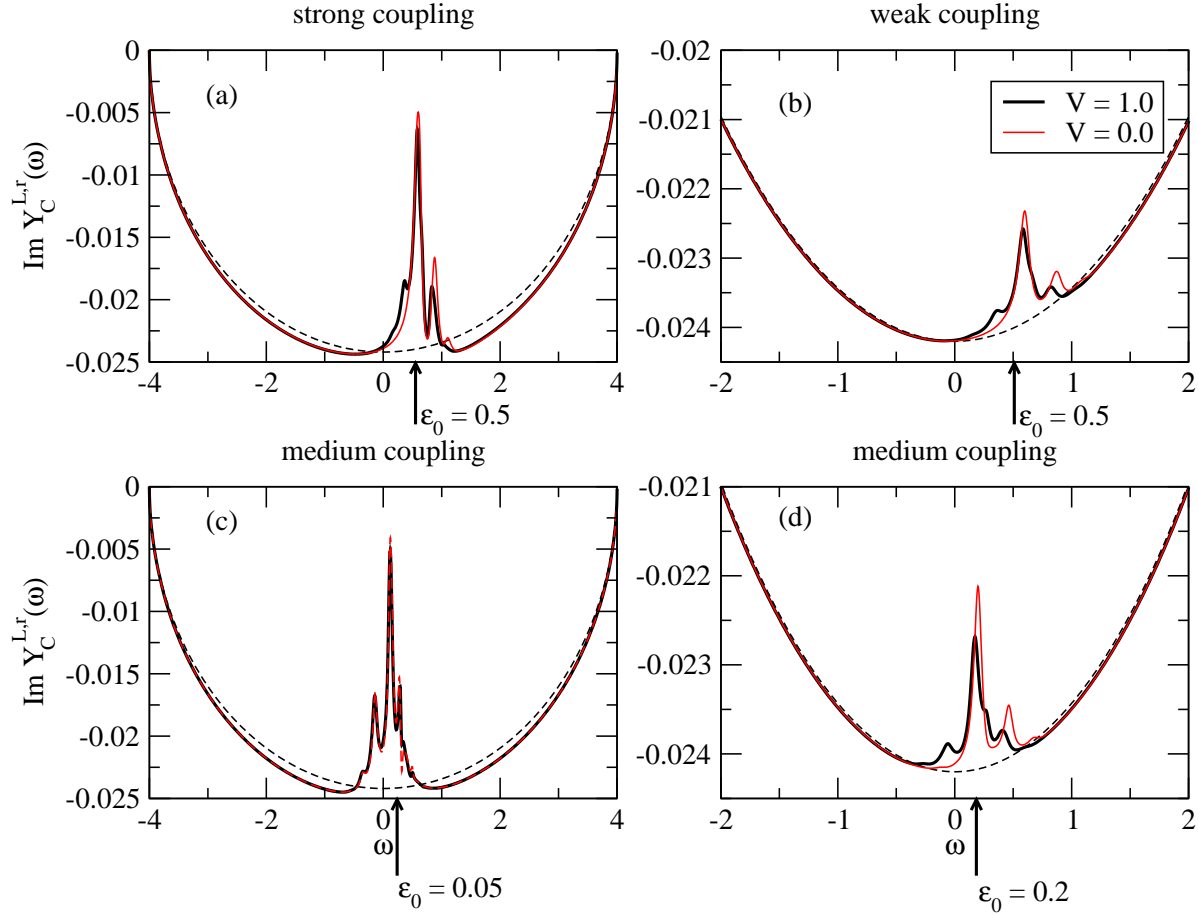


Figure 2. (Color online) Imaginary part of the left-lead generalised embedding potential $Y_C^{L,r}(\omega)$. The dashed lines represent the L lead spectral function in the absence of renormalisation at the LC interface (i.e. semi-elliptic density of states). The thin (red) lines are the spectral functions $\Im m Y_C^{L,r}(\omega)$ at equilibrium ($V = 0$). The thick (black) lines are the non-equilibrium spectral functions $\Im m Y_C^{L,r}(\omega)$ at finite bias ($V = 1.0$). These show a strong reduction of the spectral functions on energy range of $\Delta\omega \approx 1$ around ϵ_0 . Panel (a) Off-resonant regime $\epsilon_0 = 0.5$ and strong coupling at the interface $\omega_A = 0.20$, $\gamma_0 = 0.28$. (b) Off-resonant regime $\epsilon_0 = 0.5$ and weak coupling at the interface $\omega_A = 0.20$, $\gamma_0 = 0.07$. (c) Resonant regime $\epsilon_0 = 0.05$ and medium coupling at the interface $\omega_A = 0.20$, $\gamma_0 = 0.14$. (d) Intermediate regime $\epsilon_0 = 0.2$ and medium coupling at the interface $\omega_A = 0.10$, $\gamma_0 = 0.07$. The other parameters are $\omega_0 = 0.20$, $\gamma_0 = 0.15$, $t_{0R} = t_{0L} = 0.22$, $\beta_\alpha = 2.0$, $\epsilon_\alpha = 0.0$, $\eta_V = 1$.

peak in the conductance, and more importantly the lineshape of the first vibron sideband peak above the main conductance peak. The most important effects are obtained for the strong crossing interaction strength $\gamma_A = 0.28$. Even if the ratio γ_A/ω_A is conserved between the calculations shown in Figure 4 and Figure 5, the absolute value of γ_A is the crucial quantity that governs the effects of the dynamical renormalisation. Furthermore, for the different sets of parameters we have considered, our calculations show that the lower order expansion for Σ_{LC}^r (see Eq. ()) provides a good approximation to the results obtained with a larger number of levels in the continued fraction expansion

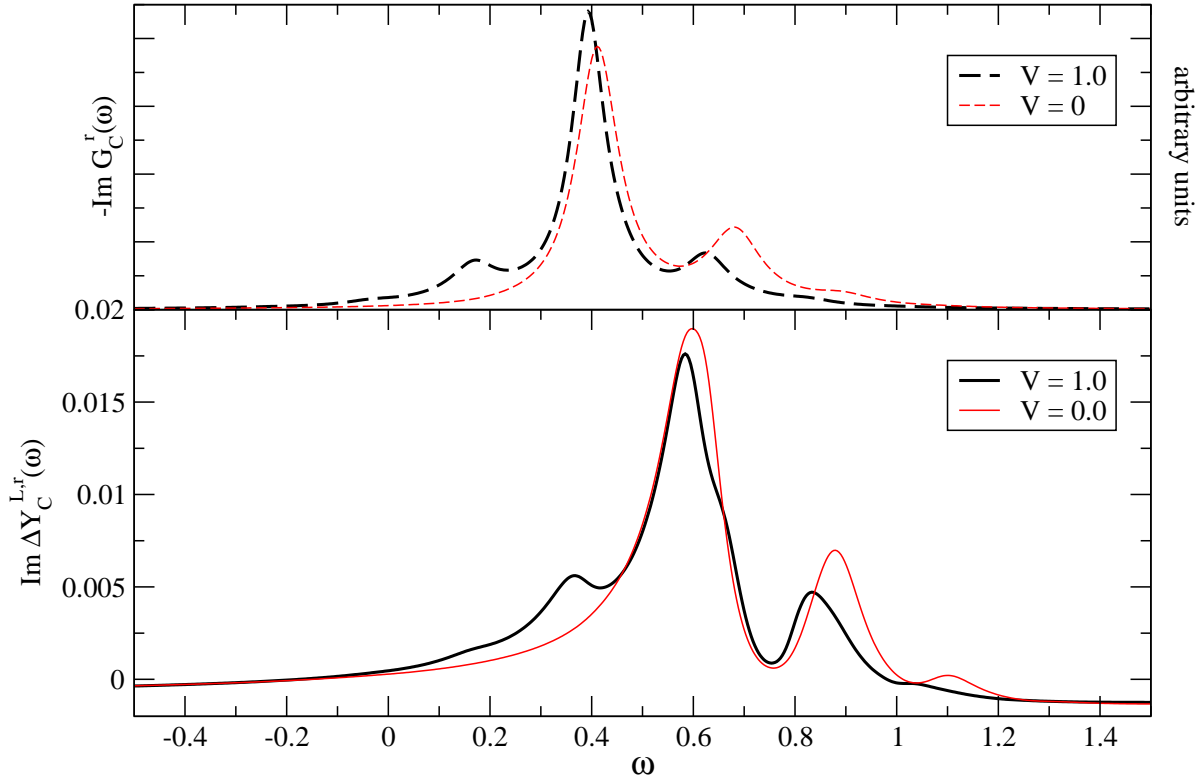


Figure 3. (Color online) Rescaled spectral function proportional to $-\Im m G_C^r$ for the central region (top panel) and imaginary part of the L lead generalised embedding potential relative to the non-renormalised L lead self-energy: $\Delta Y_C^{L,r} = Y_C^{L,r} - \Sigma_L^r$ (bottom panel). The calculations are performed for the same parameters as in panel (a) of Figure 2 and for both zero bias and finite bias $V = 1$. Here $\mu_R = 0$ and $\mu_L = V$. The qualitative correlations between the features in $\Delta Y_C^{L,r}$ and in the spectral function of the C region $-\Im m G_C^r$ are clearly observed.

of Σ_{LC}^r (see panel (a) in fig.).

We now check the effects of varying the nominal coupling $t_{0\alpha}$ on the conductance. The results are shown in Figure 6 for the off-resonant transport regime with and without dynamical renormalisation. With renormalisation of the left contact, the conductance values decrease with increasing coupling $t_{0\alpha}$ to the leads while the conductance peaks broaden. This is seen more clearly in the right panel of Figure 6 where the rescale conductance $G(V)/G_{\max}$ is plotted such that the main resonance peak has an amplitude of 1.

In the presence of dynamical renormalisation of the L contact, the main conductance peak follows the same behaviour as in the absence of renormalisation. However, one observes a highly non-linear behaviour of the modification of the first vibron side-band peak. The complete and detailed understanding of such modification is rather complex, and beyond the scope of the present paper. However it is strongly related to the new features in the renormalised L lead embedding potential which depart from the non-interacting case.

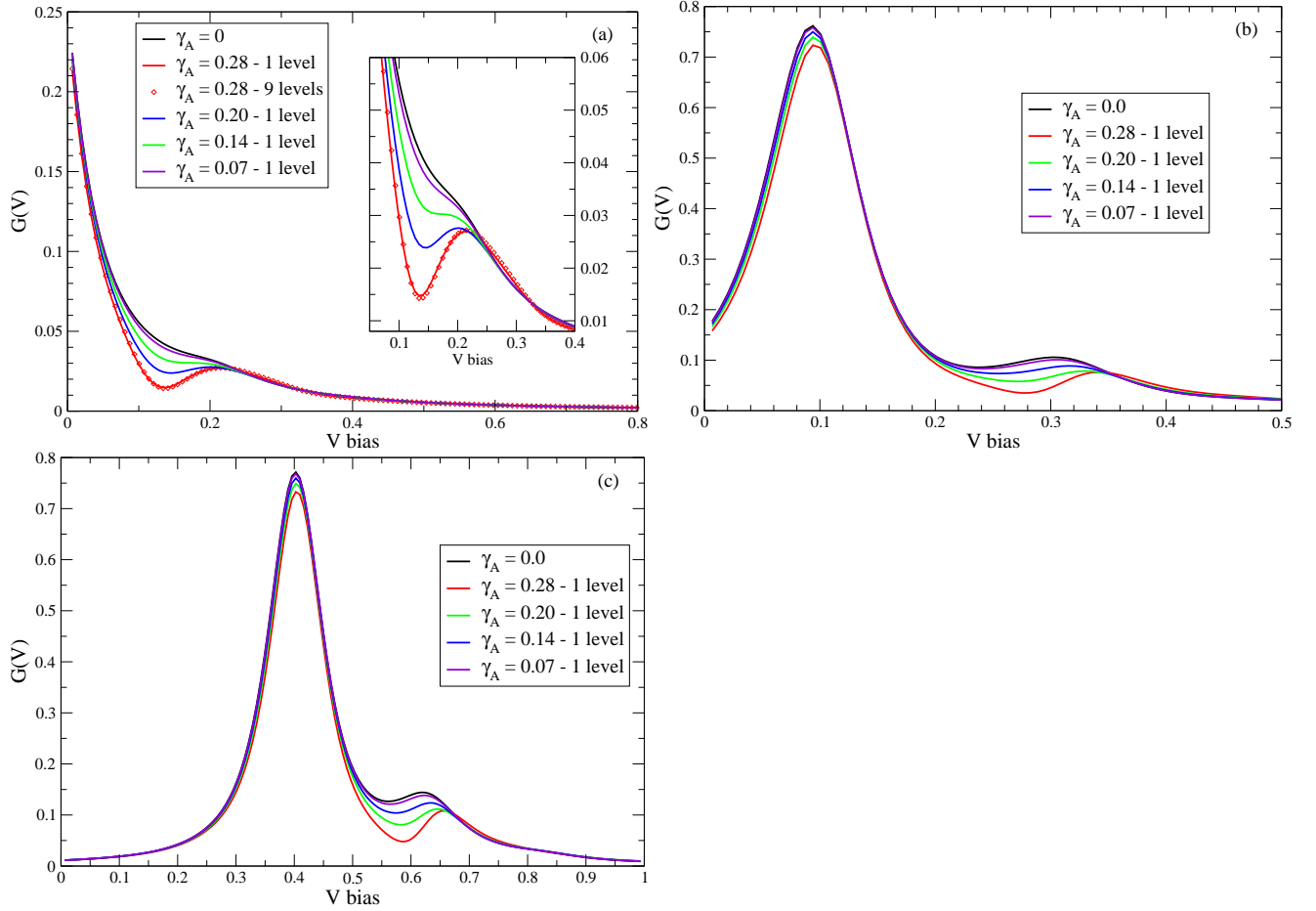


Figure 4. (Color online) Dynamical conductance $G(V)$ for different transport regimes and different coupling strength γ_A , and $\omega_A = 0.20$. Panel (a) Resonant regime $\varepsilon_0 = 0.05$. Panel (b) Off-resonant regime $\varepsilon_0 = 0.2$. Panel (c) Off-resonant regime $\varepsilon_0 = 0.5$. The non-equilibrium dynamical renormalisation of the LC contact affects both the main conductance peak and the first vibron side-band peak. The other parameters are $\omega_0 = 0.20$, $\gamma_0 = 0.15$, $t_{0R} = t_{0L} = 0.22$, $\beta_\alpha = 2.0$, $\epsilon_\alpha = 0.0$, $\eta_V = 1$.

5. Conclusion

We have studied the transport properties through a two-terminal nanoscale device with interactions present not only in the central region but also with interaction crossing at the interface between the left lead and the central region. To calculate the current for such a fully-interacting system, we have used our recently developed quantum transport formula [52] based on the NEGF formalism. As a first practical application, we have considered a prototypical single-molecule nanojunction with electron-vibron interaction. In terms of the electron density matrix, the interaction is diagonal in the central region for the first vibron mode and off-diagonal between the central region and the left electrode for the second vibron mode. The interaction self-energies are calculated in a self-consistent manner using the lowest order Hartree-Fock-like diagram in the central region and a quasi-particle (dynamical mean-field-like) approach for the

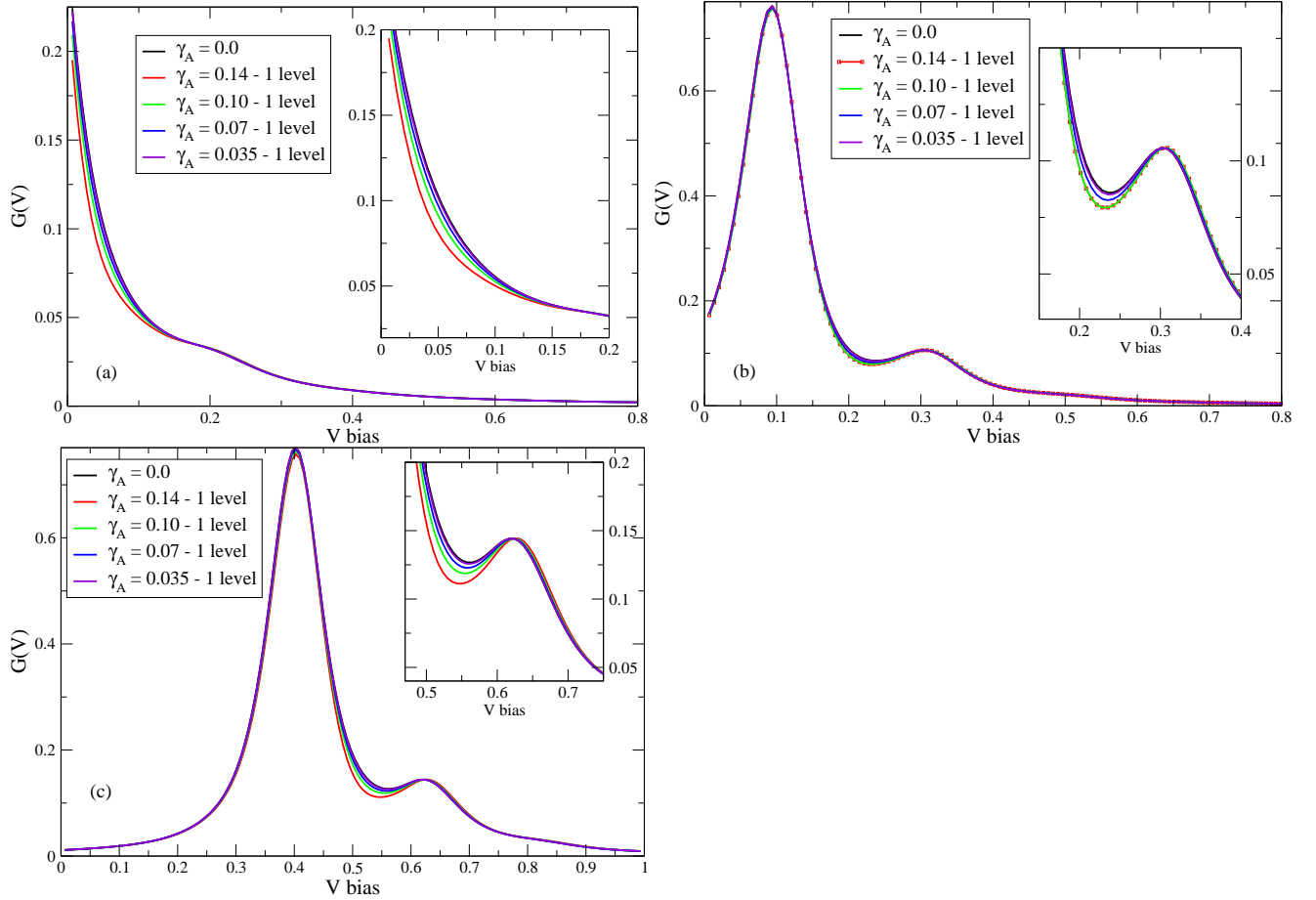


Figure 5. (Color online) Dynamical conductance $G(V)$ for different transport regimes and different coupling strength γ_A , and $\omega_A = 0.10$. Panel (a) Resonant regime $\varepsilon_0 = 0.05$. Panel (b) Off-resonant regime $\varepsilon_0 = 0.2$. Panel (c) Off-resonant regime $\varepsilon_0 = 0.5$. The non-equilibrium dynamical renormalisation of the LC contact affects both the main conductance peak and the first vibron side-band peak. The other parameters are $\omega_0 = 0.20$, $\gamma_0 = 0.15$, $t_{0R} = t_{0L} = 0.22$, $\beta_\alpha = 2.0$, $\epsilon_\alpha = 0.0$, $\eta_V = 1$.

crossing interaction. Our calculations were performed for different transport regimes ranging from the far off-resonance to the quasi-resonant regime, and for a wide range of parameter values.

They show that, for this model, we obtain a non-equilibrium (i.e. bias dependent) dynamical (i.e. energy dependent) renormalisation of the generalised embedding potential of the L left lead. The renormalisation is such that the amplitude of the corresponding spectral function is reduced around the molecular level energy ε_0 over an energy range roughly equal to the energy support of the spectral density of the central region C . This corresponds a reduction of the number of transport channels in the left lead at given energy, even if the total spectral weight of the L embedding potential is conserved.

The non-equilibrium dynamical renormalisation of the L contact is highly non-linear and non-monotonic in function of the applied bias, and the larger effects occur at

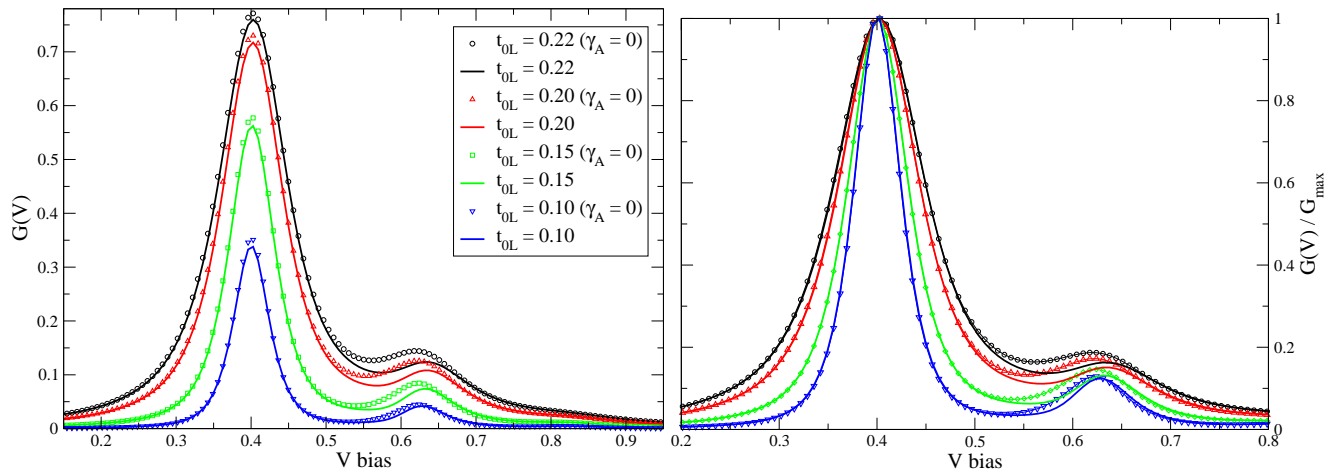


Figure 6. (Color online) (Left Panel) Dynamical conductance $G(V)$ for the off-resonant transport regime ($\varepsilon_0 = 0.50$) and different norminal coupling strength $t_{0R} = t_{0L}$ to the leads. (Right Panel) Dynamical conductance $G(V)$ rescaled such that the amplitude of the main resonance peak is 1 quantum of conductance. The other parameters are $\gamma_A = 0.2$, $\gamma_A = 0.14$ (unless otherwise indicated), $\omega_0 = 0.20$, $\gamma_0 = 0.15$, $\beta_\alpha = 2.0$, $\epsilon_\alpha = 0.0$, $\eta_V = 1$.

applied bias for which features are present in both the spectral function of the central region C and the generalised embedding potential of the L lead. The conductance is affected by the NE renormalisation of the contact: the amplitude of the main resonance peak is modified as well as the lineshape of the first vibron side-band peak.

Finally, extensions of the present study are now considered to go beyond the quasi-particle approach for the crossing interaction self-energy by including as well as the lesser and greater components of the LC interface self-energy. This should lead to dynamical NE renormalisation of the contact involving inelastic scattering processes.

References

- [1] Widawsky J R, Darancet P, Neaton J B and Venkataraman L 2012 *Nano Letters* **12** 354
- [2] Strange M, Rostgaard C, Häkkinen H and Thygesen K S 2011 *Physical Review B* **83** 115108
- [3] Rangel T, Ferretti A, Trevisanutto P E, Olevano V and Rignanes G M 2011 *Phys. Rev. B* **84** 045426
- [4] Darancet P, Ferretti A, Mayou D and Olevano V 2007 *Phys. Rev. B* **75** 075102
- [5] Baym G 1962 *Physical Review* **127** 1391
- [6] von Barth U, Dahlen N E, van Leeuwen R and Stefanucci G 2005 *Physical Review B* **72** 235109
- [7] van Leeuwen R, Dahlen N E, Stefanucci G, Almladh C O and von Barth U 2006 *Lecture Notes in Physics* **706** 33
- [8] Kita T 2010 *Progress of Theoretical Physics* **123** 581
- [9] Tran M T 2008 *Physical Review B* **78** 125103
- [10] Myöhänen P, Stan A, Stefanucci G and van Leeuwen R 2008 *EuroPhysics Letters* **84** 67001
- [11] Myöhänen P, Stan A, Stefanucci G and van Leeuwen R 2010 *Journal of Physics: Conference Series* **220** 012017
- [12] Perfetto E, Stefanucci G and Cini M 2010 *Physical Review Letters* **105** 156802
- [13] Velický B, Kalvová A and Špička V 2010 *Physical Review B* **81** 235116

- [14] von Friesen M P, Verdozzi C and Almbladh C O 2009 *Physical Review Letters* **103** 176404
- [15] Arroyo C R, Frederiksen T, Rubio-Bollinger G, Vélez M, Arnau A, Sánchez-Portal D and Agraït N 2010 *Physical Review B* **81** 075405
- [16] Ness H and Fisher A J 1999 *Physical Review Letters* **83** 452
- [17] Ness H, Shevlin S A and Fisher A J 2001 *Physical Review B* **63** 125422
- [18] Ness H and Fisher A J 2002 *Europhysics Letters* **57** 885
- [19] Mii T, Tikhodeev S and Ueba H 2003 *Physical Review B* **68** 205406
- [20] Montgomery M J, Hoekstra J, Sutton A P and Todorov T N 2003 *Journal of Physics: Condensed Matter* **15** 731
- [21] Troisi A, Ratner M A and Nitzan A 2003 *Journal of Chemical Physics* **118** 6072
- [22] Chen Y C, Zwolak M and di Ventra M 2005 *Nano Letters* **4** 1709
- [23] Lorente N and Persson M 2000 *Physical Review Letters* **85** 2997
- [24] Frederiksen T, Brandbyge M, Lorente N and Jauho A P 2004 *Physical Review Letters* **93** 256601
- [25] Galperin M, Ratner M A and Nitzan A 2004 *Nano Letters* **4** 1605
- [26] Mitra A, Aleiner I and Millis A J 2004 *Physical Review B* **69** 245302
- [27] Pecchia A, di Carlo A, Gagliardi A, Sanna S, Frauenheim T and Gutierrez R 2004 *Nano Letters* **4** 2109
- [28] Chen Z, Lü R and Zhu B 2005 *Physical Review B* **71** 165324
- [29] Ryndyk D A and Keller J 2005 *Physical Review B* **71** 073305
- [30] Sergueev N, Roubtsov D and Guo H 2005 *Physical Review Letters* **95** 146803
- [31] Viljas J K, Cuevas J C, Pauly F and Häfner M 2005 *Physical Review B* **72** 245415
- [32] Yamamoto T, Watanabe K and Watanabe S 2005 *Physical Review Letters* **95** 065501
- [33] Cresti A, Grosso G and Parravicini G P 2006 *Journal of Physics: Condensed Matter* **18** 10059
- [34] Han J E 2006 *Physical Review B* **73** 125319
- [35] Troisi A and Ratner M A 2006 *Nano Letters* **6** 1784
- [36] de la Vega L, Martín-Rodero A, Agraït N and Levy-Yeyati A 2006 *Physical Review B* **73** 075428
- [37] Frederiksen T, Paulsson M, Brandbyge M and Jauho A P 2007 *Physical Review B* **75** 205413
- [38] Galperin M, Ratner M A and Nitzan A 2007 *Journal of Physics: Condensed Matter* **19** 103201
- [39] Ryndyk D A and Cuniberti G 2007 *Physical Review B* **76** 155430
- [40] Schmidt B B, Hettler M H and Schön G 2007 *Physical Review B* **75** 115125
- [41] Troisi A, Beebe J M, Picraux L B, van Zee R D, Stewart D R, Ratner M A and Kushmerick J G 2007 *Proceedings of the National Academy of Sciences of the USA* **104** 14255
- [42] Asai Y 2008 *Physical Review B* **78** 045434
- [43] Benesch C, Čížek M, Klimeš J, Kondov I, Thoss M and Domcke W 2008 *Journal of Physical Chemistry C* **112** 9880
- [44] Paulsson M, Frederiksen T, Ueba H, Lorente N and Brandbyge M 2008 *Physical Review Letters* **100** 226604
- [45] Egger R and Gogolin A O 2008 *Physical Review B* **77** 113405
- [46] Monturet S and Lorente N 2008 *Physical Review B* **78** 035445
- [47] McEniry E J, Frederiksen T, Todorov T N, Dundas D and Horsfield A P 2008 *Physical Review B* **78** 035446
- [48] Schmidt B B, Hettler M H and Schön G 2008 *Physical Review B (Condensed Matter and Materials Physics)* **77** 165337
- [49] Secker D, Wagner S, Ballmann S, Hartle R, Thoss M and Weber H B 2011 *Physical Review Letters* **106** 136807
- [50] Härtle R, Butzin M, Rubio-Pons O and Thoss M 2011 *Physical Review Letters* **107** 046802
- [51] Ness H and Dash L K 2012 *Physical Review Letters* **108** 126401
- [52] Ness H and Dash L K 2011 *Physical Review B* **84** 235428
- [53] Perfetto E, Stefanucci G and Cini M 2012 *Physical Review B* **85** 165437
- [54] Ness H and Dash L K 2012 *Journal of Physics A: Mathematical and Theoretical* **45** 195301
- [55] Meir Y and Wingreen N S 1992 *Physical Review Letters* **68** 2512

- [56] Dash L K, Ness H and Godby R W 2010 *Journal of Chemical Physics* **132** 104113
- [57] Ness H, Dash L K and Godby R W 2010 *Physical Review B* **82** 085426
- [58] Dash L K, Ness H and Godby R W 2011 *Physical Review B* **84** 085433
- [59] Heeger A J, Kivelson S, Schrieffer J R and Su W P 1988 *Review of Modern Physics* **60** 781
- [60] Datta S, Tian W D, Hong S H, Reifenberger R, Henderson J I and Kubiak C P 1997 *Physical Review Letters* **79** 2530
- [61] Ness H and Dash L K 2012 *submitted*
- [62] Ciuchi S, de Pasquale F, Fratini S and Feinberg D 1997 *Physical Review B* **56** 4494–4512
- [63] Ness H 2006 *Journal of Physics: Condensed Matter* **18** 6307
- [64] Cini M and D’Andrea A 1988 *Journal of Physics C: Solid State Physics* **21** 193
- [65] Dash L K, Ness H, Verstraete M and Godby R W 2012 *Journal of Chemical Physics* **136** 064708